Journal of Experimental and Applied Animal Sciences
Volume 3, Number 3, pp. 151-163, 2021
Print ISSN 2314-5684 | Online ISSN 2314-5692

ORIGINAL ARTICLE

Development of an innovative zebrafish (*Danio rerio*) smear/imprint *in vitro* assay for rapid preliminary inspection of the snake venom toxinological effects

Marco Álvarez[1], Yurisbeth Zanotty[1,2], Lourdes Perdomo[1], Alexis Rodríguez-Acosta[2*]

[1]Sección de Microscopía Electrónica, Instituto Anatómico ''José' Izquierdo'', Facultad de Medicina, Universidad Central de Venezuela, Caracas, Bolivarian Republic of Venezuela.; [2]Laboratorio de Inmunoquímica y Ultraestructura, Instituto Anatómico "José Izquierdo'', Universidad Central de Venezuela, Caracas, Bolivarian Republic of Venezuela

DOI: https://doi.org/10.20454/jeaas.2021.1653

ABSTRACT

The current assay describes the implementation of an innovative animal model to investigate toxin pathology *in vivo*, with the possibility of using zebrafish larvae (*Danio rerio*) (7dpf) smear/imprint technique for preliminary inspection of snake venom activities. Molecular exclusion chromatography was done using proteins less than 30 kDa for the larvae and thus be assured that we had neurotoxins in the inoculum, since neurotoxins are generally of low molecular weight. The cuaima (*Lachesis muta muta*) venom, in addition to being neurotoxic, it is also haemorrhagic and proteolytic. Evident toxins damages were caused by the snake venom on zebrafish larvae, such as epidermal, neurotoxic and myotoxic alterations that by direct testing of a larval smear/imprint procedure they were quickly and easily demonstrated. Here was established a number of alterations, such as an obvious curvature in the caudal segment, which was accompanied by the death of the population of epidermis cells (tested by acridine orange) at the end of the larval tail; cells with highly vacuolated cytoplasm; nerve cells with a high presence of vacuolated cell bodies and irregular band pattern in the sarcomere units of muscle tissue. This method will allow to have a quick preliminary vision of the injuries that the snake venom is capable of producing in several tissues, showing in terms of time an advantage on the classical histopathological methods.

Keywords: Acridine orange staining, *Danio rerio, Lachesis muta muta,* smear/imprint technique, venom, zebrafish larvae.

INTRODUCTION

Assays for exposing snake venoms activities on different tissues have evident clinical, and experimental applications (Girón et al. 2020; Sánchez et al. 2018; Neri-Castro et al. 2020). Snake venoms are complex mixtures

of proteins and polypeptides (Tasima et al. 2020) that that besides biochemical and biological assays, they require be evidenced by histological techniques, in order to visually observing the damage generated by the various components of these venoms, which sometimes are not identifiable by conventional biochemical procedures.

Numerous attempts have been made to identify venoms by bioassay of their neurotoxic and/or myotoxic activities (Zanotty et al. 2019). Nevertheless, these assays are costly, time consuming, and sometimes nonspecific. To comprehend the action of given toxins activities, sophisticated analysis are necessary. At present histological and electron microscopy, among others, can be used to investigate such activities, but they do not allow obtaining fastest and effortlessly results. In the other hand, the use of mammalian animal models must be stopped and consequently, other animal models should be assumed. A different commonly used model relies on Zebra fish, because this fish has a genome with 80% similarity to the human.

Here, we have attempted to design an innovative smear/imprint technique (SIT) that allows, a rapid and panoramic screening of the most relevant zebrafish larva (7dpf) organs in a single sample, where structural damage can be observed at the tissue and/or cellular level that quickly guides the researcher to the target organ, where the purified toxin and/or a crude venom actions are directed (Jung et al. 2016).

This technique, not only will be useful for the study of natural toxins, such as snake venoms, scorpions, spiders and other venomous animals, but also it can be used in the description of any toxic substance, which would need to be evaluated on an ample distribution of different organs and tissues, identifying its target in all organism very quickly without needing particular tools and would be low-cost, reproducible and circumvent the use of high numbers of animals, especially mammals. It is innovative since we believe that it is an original work, which had not been done previously.

Due to scarcity of literature regarding a single snake venom poly-specific damage valuation protocols, we attempted to develop a procedure that would be comprehensive to elicit researcher's interest, as a preliminary view of toxic activity can guide the toxinologist toward the organ or tissue that would target toxic activity and save time and laboratory resources. We are using the zebrafish at the 7dpf development point, because at this stage most of the organs are matured and working.

MATERIALS AND METHODS

Venom collection. Six adult males and females of "bushmaster" (*L. muta muta*) snakes were collected at the Sierra of the Turimiquire Range (Anzoátegui, Monagas, and Sucre states, Venezuela). Its venoms were pooled at the Tropical Medicine Institute Serpentarium of the Universidad Central de Venezuela (Caracas, Venezuela). The venom was achieved by letting the snakes to bite into a disposable plastic cup covered by Para-film® (Sigma-Aldrich, St. Louis, MO, USA). Each venom sample was centrifuged in an Eppendorf Centrifuge 5430R (Eppendorf, USA) at 10,000 g for 5 min, filtered through a Millipore filtration MillexHV (Millipore, USA) unit 0.45 µm, under positive pressure, and lyophilised. They were preserved at -90^{0}C until use.

Ethical statement. Qualified personnel organised all the experimental methods relating to

the use of live animals. This work was approved by the Institute of Anatomy Ethical Committee of the Universidad Central de Venezuela on 20 January 2019 under assurance number: (#20-01-19) and followed the norms obtained from the Guidelines for the Care and Use of Laboratory Animals, published by the National Institutes of Health guide for the care and use of Laboratory animals (NIH Publications No. 8023, revised 1978) (NIH, 1985).

Chromatography purification of L. muta muta venom. Five milligrams of *Lmm* venom in 500 µL of starting buffer was run in a Sephacryl 300 size exclusion column on a chromatographic system (BIORAD, USA). Low molecular mass fractions (below 30 kDa) were selected for testing on the zebrafish larvae model.

Method to obtain zebrafish larvae. Adults and wild-type zebrafish larvae (*Danio rerio*) were cultured using a modified method (Westerfield 2007). The larvae were used 7 days after fertilization of adult fish at 28.5 °C. The larvae were placed in a microtitre with sterile fresh water solution; then, the venom was tested in the zebrafish model. Five larvae per well were placed at different venom concentrations (20 to 70 µg in 2000 µL) in sterile fresh water, as indicated below.

Morphological bioassays. Ten larvae of zebrafish (*Danio rerio*) of 7 days post-fertilization (dpf) were treated with 50 µg/2 mL of the low molecular mass fractions (<30kDa), from the *Lmm* snake venom, in order to evaluate the effects caused by the toxins and the possible signs of toxicity in tissues. For the SIT, a clean glass slide was placed on a flat surface. The experimental larvae were added to one end (as a blood smear slide is done). Then, taking another clean slide, and holding at an angle of about 45°, after squeezing the larva to break it, with one end of the slide, the larvae was running along the edge of the slide by capillary action (Figure 1). Later, the treated larvae smear was May-Grunwald Giemsa (MGG) (Sigma-Aldrich, St. Louis, MO, USA) stained, according to standard protocols. Normal control larvae were carried out by the same procedure of SIT. In this sense, the observation was carried out by determining the different organs from the zebrafish normal and envenomed larvae, using a white light microscope (Olympus BX50, USA).

Cytomorphometry. Digital images of the respective imprints, from normal controls and treated with the venom through a digital capture system were acquired (Capture IC.22. Imaging Source, The Imaging Source, LLC, USA), incorporated into an Olympus BX50 Microscope, under the objectives UPlanFl 10x/0.30 Ph1 ∞/ - and UPlanFl 100x/1.30 oil Ph3 ∞/0.17, in the number of five images per cut.

Segmentation. The segmentation processing used consisted of the application of the colour threshold to the original image stained with (MGG), and then the transformation of the product obtained, into an 8-bit binary image, white-grey-black, or mask. The regions of interest were delimited on this binary image; particularly; the vacuolization signals in the epidermal and ganglionic tissue. This was done through the definition of edges or contours around these areas, by using grayscale gradients, applying pixel intensity thresholds, and then estimating the Mean Vacuolar Area (MVA) and light-dark frequency of the muscle fibres pattern. For all that, we proceeded through the menu of the Image J Fiji program, applying Image→Adjustment→Colour

threshold→saturation of regions of inter-threshold→ delimitation of the area of interest→ analysis Tool→ ROI→ manual selection pointer→ register as area of interest by contours→ creation of the mask of the original image→ register→ measurement.

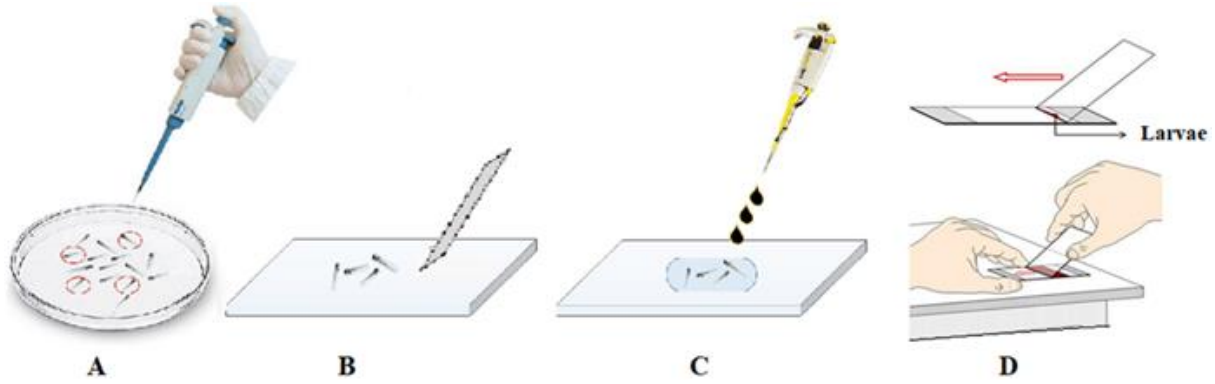

Fig. 1: Larvae envenomation and SIT explanation. (A) Larvae culture. (B) Larvae selection (7dpf) absortion of excess of water, (C) Incorporation of Lmm venom fraction (60µg/mL). (D) smear/imprint procedure.

The numerical data were obtained and analysed with a non-parametric test and were represented on a geometric graph of linear axis according to the GraphPad Prism 7.0 statistical program (GraphPad, USA). In the case of skeletal muscle fibres was made the quantification of the regularity of the striatum pattern according to fast Fourier transformations, as well as the architectural pattern of muscle fibres (Pasqualin et al. 2015). Morphological irregularities were considered and founded principally on types of modification, in addition largely categorised as early-stage injures. Analyses were triplicated as obligatory to endorse any observed damage effects. Additionally, to confirm that the toxicity was reliable and reproducible, these effects were explicitly documented as ‘‘positive’’ when observed in >80% (i.e. 8 of 10) of tested larvae. Dermal epithelium, nervous and muscles systems were analysed.

May/Grunwald Giemsa (MGG) and acridine orange staining. May Grunwald Giemsa staining was carried out according to standard protocols. For acridine orange staining, the slides were exposed during 15 min at 100 µg/mL of acridine orange solution, with a number of washes to remove the superfluous dye. Tissue images were achieved with Olympus IX-71 fluorescence microscope at an excitation wavelength of 350 nm.

Statistical analyses. The data is presented as the mean ± standard deviation of 3 independent experiments, unless otherwise specified. The significance was set at $p < 0.05$. The level of significance was $p<0.05$ for all comparisons. All analyses were performed by the GraphPad Prims software package.

RESULTS

Chromatography purification of Lmm venom. Under the size exclusion chromatography 10 fractions were obtained (data not shown). A pool from last 5 *Lmm* venom fractions, with low molecular mass < 30kDa was selected for toxicity tests, using the zebrafish larval model.

Smear/imprints of normal organs and tissues. Images from several normal organs and tissues are shown (Figure 2).

Smear/imprints of Lmm venom affected organs and tissues from zebrafish larval population (7dpf). The macroscopic evaluation revealed important changes in the anatomy of the larval population treated with the *Lmm* venom. Thus, when comparing the anatomy of the control larvae (Figure 3A), with that of the treated larvae (Figure 3B) was possible to highlight, in 80% of the treated larvae, the presence of a trunk curvature, as well as an obvious curvature at the level of caudal portion (Figure 3C), which is accompanied by the death of the epidermis cell population of the end of the larval tail, as evidenced by acridine orange (Sigma-Aldrich, St. Louis, MO, USA) assay (Figure 3D).

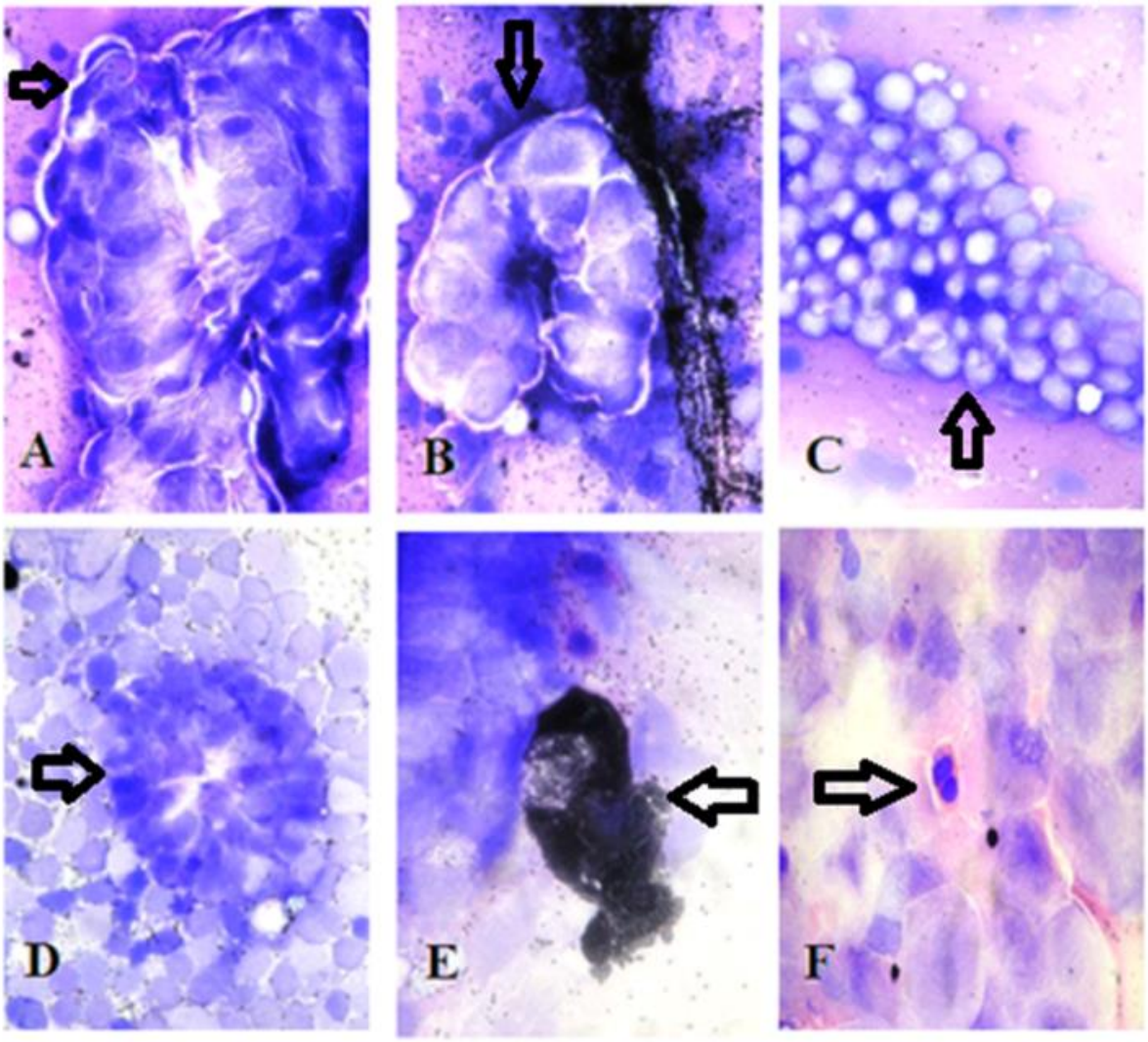

Fig. 2: Normal histological smear-imprint preparations of 7dpf zebrafish larvae (*Danio rerio*). (A) Distal or proximal kidney tubule tissue (arrow). (B) Kidney collector tubule (arrow). C) Vitelline body (arrow). (D) Neuromastoma (arrow). (E) Melanophores (arrow). (F) Mitotic body in dermal epithelium (arrow). X 100.

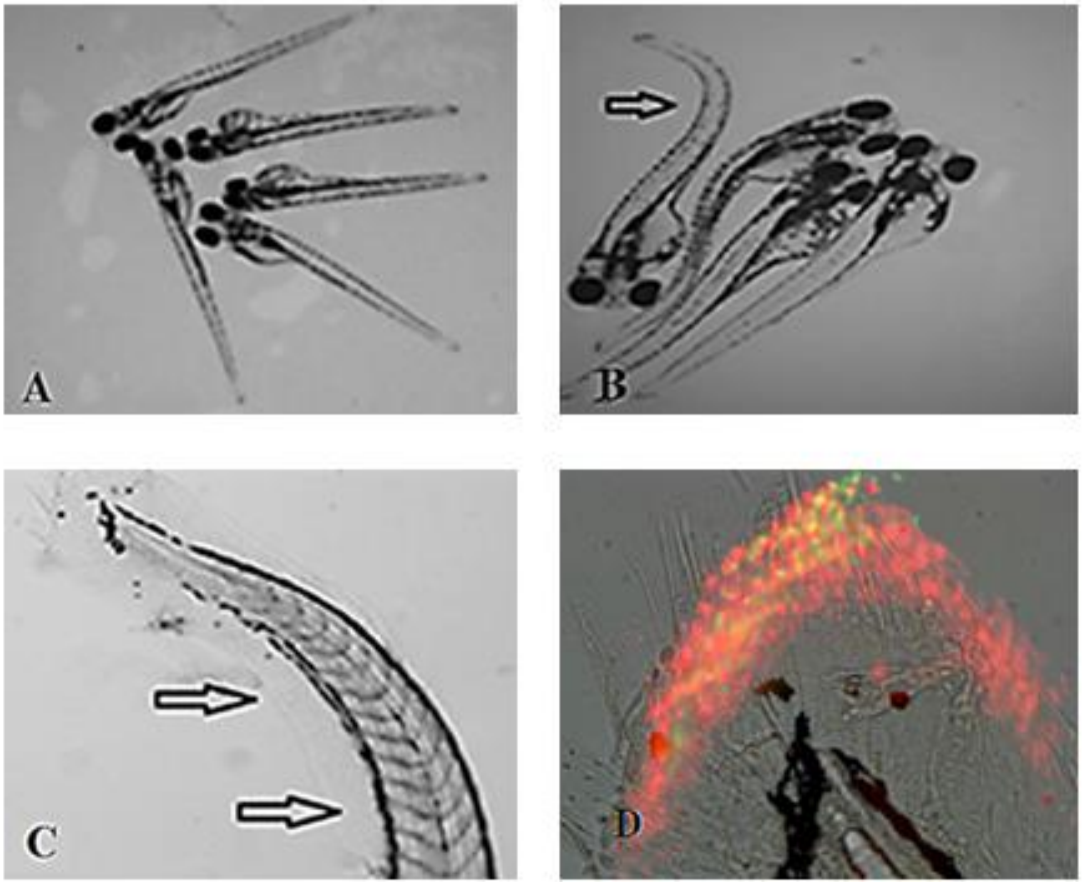

Fig. 3: Zebrafish larval population (5 dpf). (A) Normal control of whole larvae were observed. (B) Larvae treated with *Lmm* venom, the curvature of the trunk region (arrow) was noticed. (C) In the caudal region a strong curvature (arrows) was seen. (D) A robust staining with acridine orange showing apoptotic nucleus of dermal epithelium cells were observed.

Epidermal tissue. The cytohistological evaluation (MGG) and the mean vacuolar area (MVA) of the control and treated samples, in the imprints allowed to identify the characteristic footprint of epidermal epithelial tissue. Epidermal tissue regions of zebrafish larvae were recognised in the imprints, based on the appearance of epithelial monolayer of polygonal, nucleated cells with evident intercellular junctions, and intense mitotic activity (Figure 4(1-A). An epithelial monolayer, with cells with less polygonal shape, more rounded, with loss of junctions and highly vacuolated cytoplasm was identified in the imprints from zebrafish larvae treated with venom (Figure 4(1-B). Binary image analysis (Figure 4(1-C) and its morphometric quantified by the mean vacuolar area (Figure 4(1-D) were evaluated. The study of nuclear material showed a normal (Figure 4(2-A) and treated Figure 4(2-B) control larval epidermal cell segmentation. The presence of fragmentation of nuclear material and higher average nuclear area were also observed.

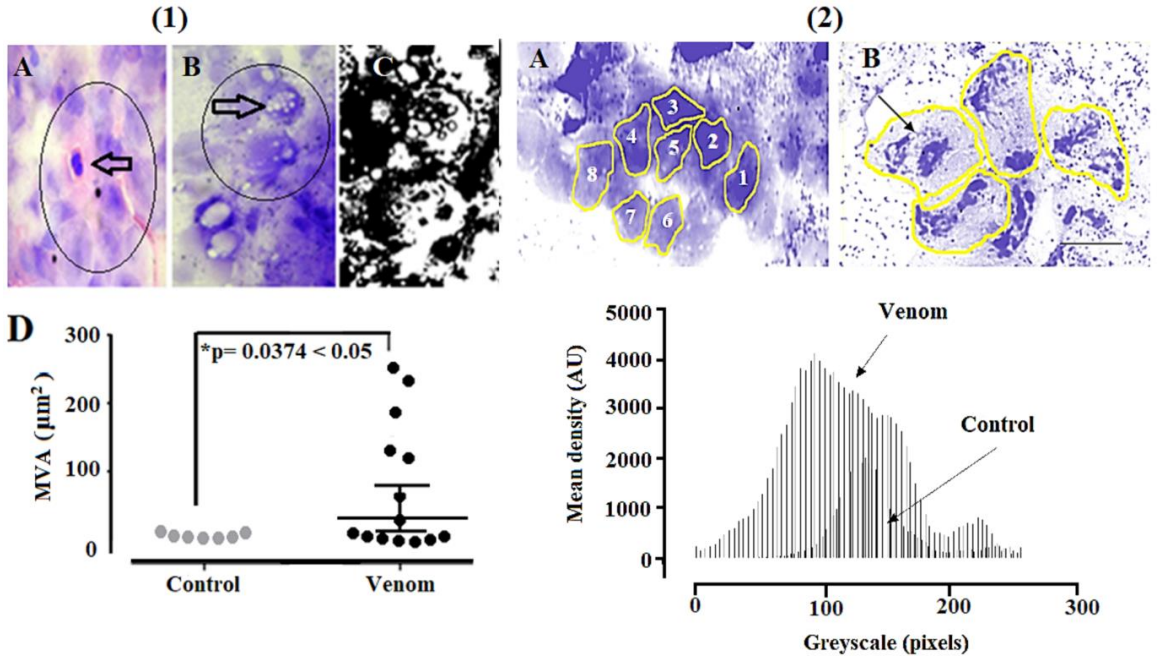

Fig. 4: Epidermal tissue. (1): (A) Epidermal tissue regions of normal zebrafish larvae were recognised in the imprints, based on the appearance of epithelial monolayer of polygonal, nucleated cells displaying evident intercellular junctions (circle), and intense mitotic activity (arrow). (B) An epithelial monolayer showing cells with less polygonal shape, more rounded, with loss of junctions (circle) and highly vacuolated cytoplasm (arrows) were identified in the smear/imprints from zebrafish larvae treated with *Lmm* venom. (C) Binary image analysis and (D) its morphometric were quantified by the mean vacuolar area (MVA) from control and venom values. X 100. (2): Normal (A) and treated (B) control larval epidermal cell segmentation. The presence of fragmentation of nuclear material (arrow) and higher average nuclear area (graph) were observed. AU: arbitrary units. Bar = 0.012 µm.

Nervous tissue. Regions of nerve tissue of zebrafish larvae were recognized by SIT, based on the microarchitecture, formed by clusters of obvious cell bodies sending filamentous projections, like strongly coloured nerve projections (Figure 5(1-A). Microarchitecture of similar conformation was recognised in smear/imprints from larvae treated with venom, however, with a high presence of vacuolated cell bodies (Figure 5(1-B). Binary image analysis (Figure 5(1-C) and its morphometric were quantified by the mean vacuolar area (Figure 5(1-D). Control (Figure 5(2-A) and treated (Figure 5(2-B) nerve fibre segmentation were evaluated. The existence of numerous vacuoles in addition to the vacuolar distribution were highlighted.

Muscular tissue. Regions of normal skeletal muscle tissue of zebrafish larvae were recognised in the imprints based on the obvious morphology of striated fibre, with a pattern of bands along the fibres and sarcomeres highlighting the Z bands (Figure 6(1-A). Evident striated fibre morphology was identified in smear/imprints from larvae treated with the venom, however, these images showed irregular band pattern in the sarcomere units (Figure 6(1-B). The analysis of the respective binary images (Figure 6(1-C) and their morphometric confirmed this (Figure 6(1-D). The segmentation of the striation pattern of the normal control of muscle fibre (Figure 6(2A) and venom treated (Figure 6(2-B) were estimated. Change based on different grey-scale histogram pattern is shown.

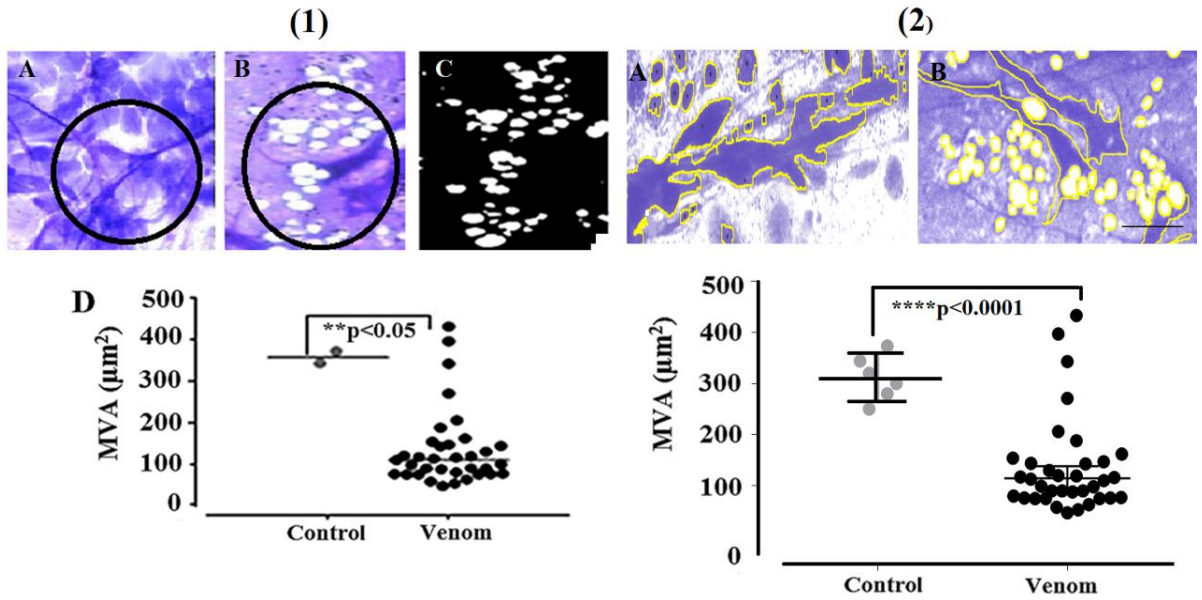

Fig. 5: Nerve tissue imprints. (1-A) Regions of normal tissue nerves of zebrafish larvae formed by clusters of obvious cell bodies sending filamentous projections, like strongly stained nerve projections (oval) in the imprints were recognised. (1-B) Microarchitecture of similar conformation was identified in smear/imprints of larvae treated with *Lmm* venom, but with a high presence of vacuolated cell bodies (circle). (1-C) Binary image analysis and (1-D) its morphometric were quantified by the mean vacuolar area (MVA) from control and venom values. X100. (2) Control (A) and treated (B) nerve fibre segmentation. The presence of numerous vacuoles (arrow) as well as the vacuolar distribution (graph) are highlighted. Bar = 0.012 µm.

Cytomorphometry. This allowed quantifying the different signs of observed damage. Thus, the Mean Vacuolar Area (MVA), in the representative traces of the epidermal tissues, muscle and nerve tissue smear/imprints could be quantified (Figures 4 and 5). Vacuolar larger values were recorded in the ganglion cell layer compared to values of vacuolar size recorded in epidermal tissue cells, with a statistical significance of values of * p <0.05 and ** p> 0.05 respectively (Figures 4 and 5). The apparent interruptions in the sarcomeric assembly recorded in the representative trace of the muscle tissue of those treated with venom, resulted in a loss of refringence, characterised by a loss of frequency in the black white pattern recorded by image analysis, and the numerically lower value of this frequency compared to the control (Figure 6(1A and 1B).

DISCUSSION

At present, the possibility of evaluating tissue lesions in the different organs of animals envenomed by toxins present in snake venoms or other toxin-producing animals, requires significant amounts of *in vivo* and *in vitro* cumbersome methods, and also expensive laboratory reagents. Reviewing the *status quo* of techniques such as histopathology, which requires fastidious handling processes, such as paraffin inclusion, cuts and staining in some cases, with special colorations: in other cases, handling and slaughter of small mammals or other animals, as well as other more sophisticated methodologies, such as electron microscopy, we are proposing here, the use of a quick and cheap test, to see damage in zebra fish larvae caused by snake venom. All of the mathematical calculations were carried out, to demonstrate that the findings of tissue altera-

tions were measurable and certain. Whoever does the technique does not need to make these calculations, if not just see that the alterations are real.

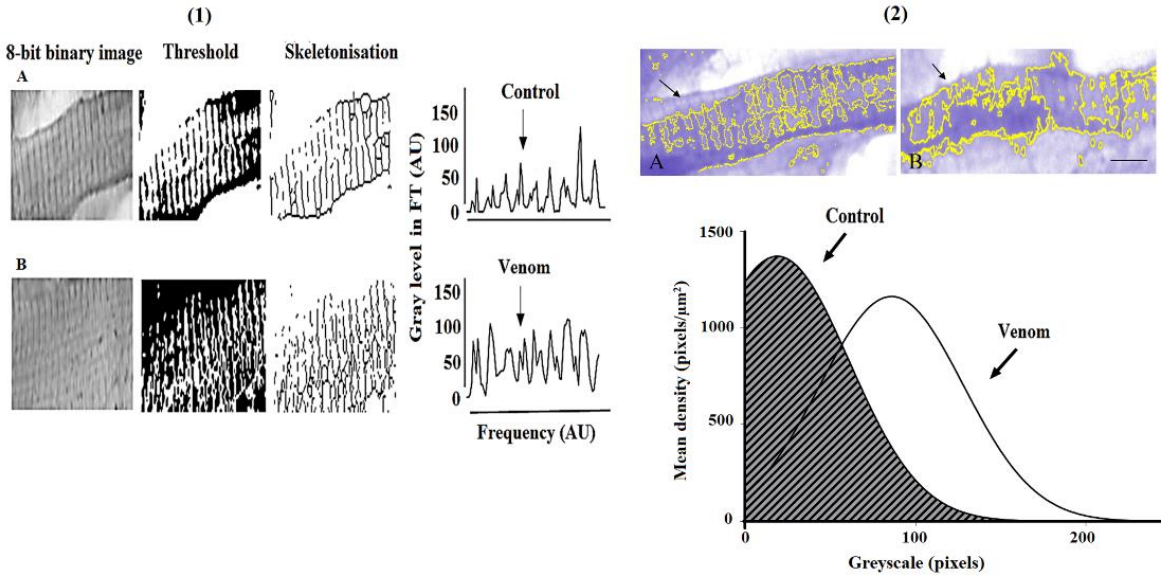

Fig. 6: Muscle tissue imprints. (1) Images (1-A) and (1-B) were obtained from the control imprint and venom respectively with equal brightness level. An automatic threshold was applied to both images before skeletonisation. The skeletons of images (1-A) and (1-B) are shown on the right with their corresponding spectrum profiles in transformations of the peaks representing the level of the tubules t organisation. AU: arbitrary units. FT: fibrous tissue. **(2)** Segmentation of the striation pattern of the normal control of muscle fibre (2-A) and venom treated (2-B) was evaluated. Change based on different grey-scale histogram pattern (arrows) was noticed. Bar = 0.012 µm.

For first identification targets, these methods could be postponed to perform more sophisticated histopathological studies, by using fish larvae, in an early stage of development, which are very easy to obtain. We wish to propose in this work a test of undemanding and fast execution, to make a quick screening to locate lesions in organs, and from there, at the site of the altered tissue starting from this rapid panoramic view tests that are more refined. This quick view places us, at the site of the damaged tissue, and later we can extrapolate to higher organisms, such as humans or mammals in general (which share a great affinity in their genomes, with these fish), the location of the toxins targets that we want to explore.

In the current paper has been used low molecular masses toxins from the "bushmaster" (*Lmm*) snake venom. In Venezuela *Lmm* species lives in the Sucre, Bolivar, Amazonas, Monagas and Delta Amacuro states (Rengifo and Rodriguez-Acosta, 2019). Myotoxic, cardiotoxic, fibrinolytic, haemorrhagic and platelet function activities have been detected in the fractions of this venom (Zanotty et al. 2019), which showed a high number of protein bands determined by 15% sodium dodecyl sulphate-polyacrylamide gel electrophoresis (SDS-PAGE) (data not shown).

Zebrafish embryos are permeable to toxins, offering straightforward access for toxin dispensation and vital dye staining. These embryos can without difficulty be handled using well-established protocols (Zanotty et al. 2019; Stednitz and Washbourne, 2020) as a rule, main organs include the stomach, intestine and the vasculature are in position by 2

days' post-fertilisation, and embryogenesis is entire 7 days after fertilisation. Embryos are optically translucent, a feature that simplifies direct examination of internal organs by light microscopy.

Comparing imprints of normal zebrafish larvae tissue was possible to observe the presence of a set of alterations, on different organs and tissues of the larvae treated by contact, with sublethal doses of this venom. The normal tissues figure was included, in order to see the organ and tissue images can be identified in a simple smear/imprint.

The epidermis-stratified epithelium was characterised by large cells in tight junctions and intense proliferative activity, as evidenced by the numerous mitotic figures. Epitheliums offer an essential defending wall for our body structures and are similarly the places where several snake venoms act too. Here, we present the developing zebrafish epidermis as a remarkable model system for studying venom damage on mitotic epithelial cells (Jevtov et al. 2014). Visualisation of how damages in mitosis lead to developmental disorders will significantly increase understanding of the pathogenesis of snakebite envenomation. Mitosis is decisive for living thing growth and differentiation. The activity is extremely effective and involves well-organised actions to achieve appropriate microtubule-kinetochore connection, chromosome segregation and chromatin condensation. Toxin actions in this refined process can end in health damages processes (Percival and Parant, 2016; Sinna et al. 1992).

In the current work, detecting epidermal tissue in the normal control imprints, the stratified epithelium was characterised by large cells in narrow junctions; an intense proliferative activity was highlighted, as evidenced by the numerous mitotic figures. Unlike, the smear/imprints affected by the venom, smaller cells were obvious with loss of tight junctions, proliferative activity and intense vacuolisation. The presence of fragmentation of nuclear material and higher average nuclear area as sign of intense damages were observed. When performing an acridine orange staining, a strong staining fluorescence in the nucleus of the caudal cells caused by *Lmm* venom was highlighted.

Lachesis muta muta venom triggered expressive morphological alterations in muscle tissues. The transverse tubule system in mammalian striated muscle is extremely structured and supports to best and standardised contraction (Sonal et al. 2014). Scarce instruments have been described for the quantification of the t-tubule system organisation in muscle tissues from snake envenomed patients. Light microscopy exhibited that the intensity of alterations exposed by muscle fibres correlated with the venom concentrations used. In the zebrafish normal controls, the muscle fibres stand out without interruptions in the sarcomeres assembly, as well as a regular bright birefringence indicative of highly organised muscles in the larvae at 7 dpf. In contrast, after 30 min of incubation with 50 µg of venom, the envenomed zebrafish larvae muscle morphology displayed fibres with pronounced heterogeneity in size, several of which demonstrated double the size and others smaller the size of the fibres of normal control muscles. Such variance in the fibres was a result of the presence of oedematised fibres and small fibres that have missed part of the myofibrils content, possibly as result of phospholipases and proteolytic activities of the venom. The muscle affected by the venom also showed prominent irruptions, alterations of

smaller cells, with loss of tight junctions, proliferative activity and an intense vacuolisation. Furthermore, the muscle fibres sections that were properly noticeable in control samples, turn lesser organised in venom-treated preparations. So, one of the mostly affected tissues was the skeletal muscle, where great vacuolisation was observed, a fact that had already been described in electron microscopy work using Viperidae venom (Tu and Morita, 1983). These lesions were characterised by myonecrosis through widespread vacuolisation of the sarcoplasmic reticulum (Ponce-Soto et al. 2010). Segmentation of the striation pattern of the normal control of muscle fibre (2-A) and venom treated was evaluated showing profound differences, which were demonstrated with the different grey-scale histogram patterns. The diffuse character of this damage may be the consequence of the phospholipids and specific proteases actions on the cellular membrane, as above proposed. The α-myotoxins occurring in Viperidae venoms and other peptides work mutually with sodium channels, rising sodium influx and causing myofibril necrosis, which is the product of the action of different basic toxins in the venom, such as the phospholipase A_2. On the other hand, these toxins do not always employ their catalytic activity on the muscle fibre, but they can induce calcium influx effects occasioning permanent tissue injury (Gasanov et al. 2011).

Observing nervous tissues, no changes were observed in the normal control sample, where normal cell structures appeared to be intact. In divergence, the snake venom caused structural changes in the central and peripheral nervous system (PNS) in the analysed group; damage to the ganglions cells were clearly visible under the optical microscope, these cells showed signs of an evident process of vacuolisation in the treated samples.

Zebrafish larvae have significant benefits in the evaluation of neurotoxicity, and represent an excellent *in vivo* model in this area (Garcia and Noyes, 2016; Kalueff et al. 2016). The zebrafish nervous system discloses several common characteristics with mammals, involving extensive anatomical features, such as the presence of the cerebellum, telencephalon, diencephalon, spinal cord and autonomic enteric nervous systems (Wullimann and Mueller, 2004; Guo, 2004; Schmidt et al. 2013). The central nervous system (CNS) development of the zebrafish larva take place within the first three days after fertilisation; and it has a high degree of genetic, morphological and physiological homology with humans (Mueller et al. 2006). It was expected, that the actions on the synaptic membrane by the proteolytic toxic processes of the *Lmm* venom, would damage the synaptic transmission of the nervous and muscular structures.

The study of the zebrafish vitelline body is an exceptional example, for detection of toxins disorders to primary embryonic nourishment, and have utility to discern systematic insights into the developmental origins of damages (Mizell and Romig, 1997). One of the best direct via where toxins affect maternal yolk deposition, is through disturbance of maternal vitellogenin production (Mizell and Romig, 1997).

CONCLUSIONS

The SIT was useful for preliminary inspection of snake venom activities. The numerous toxic actions and easily demonstrable epithelial, myotoxic and neurotoxic damages were evident and induced rapid, with a single larval smear procedure, re-enhanced with an added value provided by the quantitative data of toxic damage through image analysis. As far as we know, these results characterised a

novel technique for describing the damage in zebrafish tissue caused by *Lmm*.

FUNDING AND ACKNOWLEDGMENTS

This research did not receive any specific grant from funding agencies in the public, commercial, or not-for-profit sectors. Thanks to the Herpetologist Luis. F. Navarrete for the snake venom donation.

DISCLOSURE STATEMENT

The author declares no conflicts of interest.

REFERENCES

Abu Sinna G, al-Zahaby A, Abd el-Aal A, Abd el-Baset A, Saber T. Short term effects of animal venoms on the mitotic index of the duodenal mucosa of albino rats. Nat Toxins. 1992; 1(2):111-118.

Garcia GR, Noyes PD, Tanguay RL. Advancements in zebrafish applications for 21st century toxicology. Pharmacol Ther. 2016; 161:11-21.

Gasanov SE, Dagda RK, Rael ED. Snake Venom Cytotoxins, Phospholipase A_2S, and Zn^{2+}-dependent Metalloproteinases: Mechanisms of Action and Pharmacological Relevance. J Clin Toxicol. 2014; 4(1):1000181.

Girón ME, Ramos MI, Cantillo AC, Oramas JA, Sánchez EE, Jiménez JC, Suntravat M, Rodríguez-Acosta A. Haemostatic and biological activities of the uracoan rattlesnake (Crotalus vegrandis Klauber 1941) venom: isolation of a new snaclecs-like uracolectin with coagulant activity. SABER Universidad de Oriente, Venezuela 2020; 32:22-33.

Guo S. Linking genes to brain, behavior and neurological diseases: what can we learn from zebrafish? Genes Brain Behav. 2004; 3(2):63-74.

Jevtov I, Samuelsson T, Yao G, Amsterdam A, Ribbeck K. Zebrafish as a model to study live mucus physiology. Sci Rep. 2014; 4:6653.

Jung HM, Isogai S, Kamei M, Castranova D, Gore AV, Weinstein BM. Imaging blood vessels and lymphatic vessels in the zebrafish. Methods Cell Biol. 2016; 133:69-103.

Kalueff AV, Echevarria DJ, Homechaudhuri S, Stewart AM, Collier AD, Kaluyeva AA, Li S, Liu Y, Chen P, Wang J, Yang L, Mitra A, Pal S, Chaudhuri A, Roy A, Biswas M, Roy D, Podder A, Poudel MK, Katare DP, Mani RJ, Kyzar EJ, Gaikwad S, Nguyen M, Song C; International Zebrafish Neuroscience Research Consortium ZNRC. Zebrafish neurobehavioral phenomics for aquatic neuropharmacology and toxicology research. Aquat Toxicol. 2016; 170:297-309.

Mizell M, Romig ES. The aquatic vertebrate embryo as a sentinel for toxins: zebrafish embryo dechorionation and perivitelline space microinjection. Int J Dev Biol. 1997; 41(2):411-423.

Mueller T, Vernier P, Wullimann MF. A phylotypic stage in vertebrate brain development: GABA cell patterns in zebrafish compared with mouse. J Comp Neurol. 2006; 494(4):620-634.

Neri-Castro E, Bénard-Valle M, Archundia I, Calvete JJ, Alagón A. Implications of snake venom variation on antivenom neutralization: The case of North American vipers. Toxicon. 2020; 177 (Suppl 1):S25.

NIH. Principles of Laboratory Animal Care, vol. 85. National Institute of Health, USA 1985:pp. 1–112.

Pasqualin C, Gannier F, Malécot CO, Bredeloux P, Maupoil V. Automatic quantitative analysis of t-tubule organization in cardiac myocytes using ImageJ. Am J Physiol Cell Physiol. 2015; 308(3):C237-245.

Percival SM, Parant JM. Observing Mitotic Division and Dynamics in a Live Zebrafish Embryo. J Vis Exp. 2016; (113):e54218.

Ponce-Soto LA, Martins-de-Souza D, Marangoni S. Neurotoxic, myotoxic and cytolytic activities

of the new basic PLA(2) isoforms BmjeTX-I and BmjeTX-II isolated from the Bothrops marajoensis (*Marajó Lancehead*) snake venom. Protein J. 2010; 29(2):103-113.

Rengifo C, Rodríguez-Acosta A. Serpientes, venenos y su tratamiento en Venezuela. Caracas, Venezuela: Fondo de Publicaciones de la Facultad de Medicina de la Universidad Central de Venezuela. 2019.

Sánchez EE, González R, Lucena S, García S, Finol HJ, Suntravat M, Girón ME, Fernández I, Rodríguez-Acosta A. Crotamine-like from Southern Pacific rattlesnake (Crotalus oreganus helleri) Venom acts on human leukemia (K-562) cell lines and produces ultrastructural changes on mice adrenal gland. Ultrastruct Pathol. 2018; 42(2):116-123.

Schmidt R, Strähle U, Scholpp S. Neurogenesis in zebrafish - from embryo to adult. Neural Dev. 2013; 8:3.

Sonal SJ, Phatak M, Banerjee S, Mulay A, Deshpande O, Bhide S, Jacob T, Gehring I, Nuesslein-Volhard C, Sonawane M. Myosin Vb mediated plasma membrane homeostasis regulates peridermal cell size and maintains tissue homeostasis in the zebrafish epidermis. PLoS Genet. 2014; 10(9):e1004614.

Stednitz SJ, Washbourne P. Rapid Progressive Social Development of Zebrafish. Zebrafish. 2020; 17(1):11-17.

Tasima LJ, Hatakeyama DM, Serino-Silva C, Rodrigues CFB, de Lima EOV, Sant'Anna SS, Grego KF, de Morais-Zani K, Sanz L, Calvete JJ, Tanaka-Azevedo AM. Comparative proteomic profiling and functional characterization of venom pooled from captive Crotalus durissus terrificus specimens and the Brazilian crotalic reference venom. Toxicon. 2020; 185:26-35.

Tu AT, Morita M. Attachment of rattlesnake venom myotoxin a to sarcoplasmic reticulum: peroxidase conjugated method. Br J Exp Pathol. 1983; 64(6):633-637.

Westerfield M. The Zebrafish Book, 5th Edition; A Guide for the Laboratory Use of Zebrafish (Danio rerio). Eugene OR, USA: University of Oregon Press 2007.

Wullimann MF, Mueller T. Teleostean and mammalian forebrains contrasted: Evidence from genes to behavior. J Comp Neurol. 2004; 475(2):143-162.

Zanotty Y, Álvarez M, Perdomo L, Sánchez EE, Giron ME, Jimenez JC, Suntravat M, Guerrero B, Ibarra C, Montero Y, Medina R, Navarrete LF, Rodríguez-Acosta A. Mutacytin-1, a New C-Type Lectin-Like Protein from the Venezuelan Cuaima (*Lachesis muta muta* Linnaeus, 1766) (Serpentes: Viperidae) Snake Venom Inducing Cardiotoxicity in Developing Zebrafish (*Danio rerio*) Embryos. Zebrafish. 2019; 16(4):379-387.

Received 21 Feb 2021
Accepted 29 Mar 2021
Corresponding author:
Dr. Alexis Rodríguez-Acosta
Immunochemistry and Ultrastructural Laboratory
Anatomical Institute
Universidad Central de Venezuela
Ciudad Universitaria de Caracas
Bolivarian Republic of Venezuela
Tel: +58(212) 4917243
E-mail: rodriguezacosta1946@yahoo.es